Crack initiation life in notched Ti-6Al-4V titanium bars under uniaxial and multiaxial fatigue: synthesis based on the averaged strain energy density approach

Giovanni Meneghetti, Alberto Campagnolo
University of Padova, Department of Industrial Engineering, Padova (Italy)
giovanni.meneghetti@unipd.it alberto.campagnolo@unipd.it

Filippo Berto
University of Padova, Department of Management and Engineering, Vicenza (Italy)
NTNU, Department of Engineering Design and Materials, Trondheim, (Norway)
berto@gest.unipd.it

Keisuke Tanaka
Meijo University, Department of Mechanical Engineering, Nagoya (Japan)
ktanaka@meijo-u.ac.jp

ABSTRACT. The fatigue behaviour of circumferentially notched specimens made of titanium alloy, Ti-6Al-4V, has been analysed. To investigate the notch effect on the fatigue strength, pure bending, pure torsion and multiaxial bending-torsion fatigue tests have been carried out on specimens characterized by two different root radii, namely 0.1 and 4 mm. Crack nucleation and subsequent propagation have been accurately monitored by using the direct current potential drop (DCPD) technique. Based on the results obtained from the potential drop technique, the crack initiation life has been defined in correspondence of a relative potential drop increase $\Delta V/\Delta V_0$ equal to 1%, and it has been used as failure criterion. Doing so, the effect of extrinsic mechanisms operating during crack propagation phase, such as sliding contact, friction and meshing between fracture surfaces, is expected to be reduced. The experimental fatigue test results have been re-analysed by using the local strain energy density (SED) averaged over a structural volume having radius R_0 and surrounding the notch tip. Finally, the use of the local strain energy density parameter allowed us to properly correlate the crack initiation life of Ti-6Al-4V notched specimens, despite the different notch geometries and loading conditions involved in the tests.

KEYWORDS. Titanium alloy; Fatigue notch effect; Potential drop method; Crack initiation; Averaged SED.

Citation: Meneghetti, G., Campagnolo, A., Berto, F., Tanaka, K., Crack initiation life in notched Ti-6Al-4V titanium bars under uniaxial and multiaxial fatigue: synthesis based on the averaged strain energy density approach, Frattura ed Integrità Strutturale, 41 (2017) 8-15.

Received: 10.03.2017
Accepted: 15.04.2017
Published: 01.07.2017

INTRODUCTION

In the recent literature [1–6], an unexpected notch-strengthening phenomenon was found in circumferentially notched specimens under pure torsion or combined tension-torsion multiaxial fatigue loadings. The fatigue life of notched bars resulted longer than that of smooth ones, the higher the stress concentration factor under the same load amplitude. This notch-strengthening effect has been observed by fatigue testing cylindrical specimens made of austenitic stainless steels [1–3], NiCrMo steel [4], pure titanium [5], but it was not found in carbon steels [3,7,8]. As recently discussed by Tanaka [6], this effect can be explained on the basis of different morphologies of the fracture surfaces: in circumferentially notched bars under torsion fatigue loadings, factory-roof type fracture surfaces have been found; consequently, the sliding contact and the meshing between crack surfaces cause the retardation of crack propagation [9–13].

In this context, the fatigue behaviour of circumferentially notched specimens made of titanium grade 5 alloy, Ti-6Al-4V, has been analysed in the present contribution. To investigate the effect of the notch geometry and the loading condition on the fatigue strength of the titanium alloy, pure bending, pure torsion and multiaxial bending-torsion fatigue tests have been carried out on specimens characterised by two different notch root radii ρ, namely 0.1 and 4 mm. In all cases, the nominal load ratio R has been kept constant and equal to -1. Crack initiation and subsequent propagation have been accurately monitored by using the Matelect® DCM-2 direct current potential drop (DCPD) method, which allows to define the crack initiation life in correspondence of an increase of the electrical potential drop.

The experimental fatigue results have been re-analysed by using the local strain energy density (SED) averaged over a structural volume having radius R_0 surrounding the notch tip, as proposed by Lazzarin and Zambardi [14] and Lazzarin and Berto [15]. According to a recent contribution [16], to exclude all extrinsic mechanisms acting during the fatigue crack propagation phase, such as sliding contact, friction and meshing between mating crack surfaces, the crack initiation life has been considered.

For the sake of brevity and the experimental fatigue tests being ongoing, in this contribution the preliminary experimental fatigue results only relevant to pure bending loading will be discussed and reanalyzed.

EXPERIMENTAL FATIGUE TESTS

The geometry of the fatigue tested bars, made of Ti-6Al-4V titanium alloy, is reported in Fig. 1, along with details of the circumferential notches characterized by different values of the notch tip radius ρ.

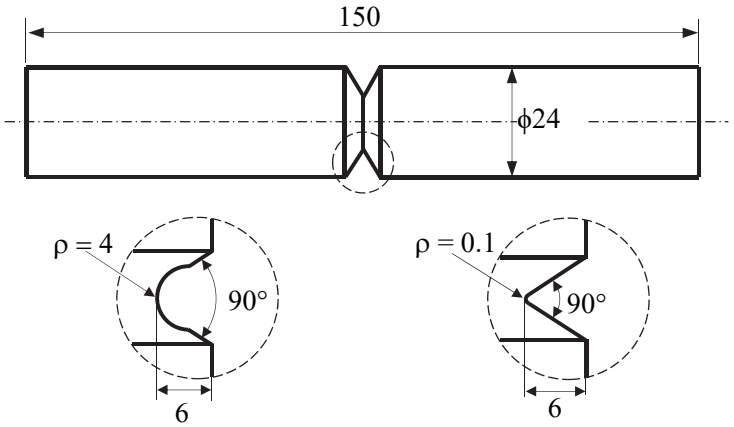

Figure 1: Geometry of the circumferentially notched specimens (dimensions are in mm).

The experimental fatigue tests have been carried out by means of a flexible test bench: with the experimental arrangement shown in Fig. 2a it has been possible to execute fatigue tests under pure bending, pure torsion and combined bending-torsion loadings by properly setting the external loads applied to the specimen by two independent hydraulic actuators. A nominal load ratio R equal to -1 has been adopted in all fatigue tests.

In all fatigue tests, the Matelect® DCM-2 direct current potential drop method, sketched in Fig. 2b, has been adopted to monitor in detail both fatigue crack initiation and propagation phases. Two specimens have been used: one was the fatigue

tested specimen, while the other one was the reference unloaded specimen. The specimens were connected in series so that a 30-A-constant-current (I in Fig. 2a) flowed through both of them.

During each experimental fatigue test, the electrical potential drops ΔV, for the tested specimen, and ΔV_0, for the reference one (see Fig. 2b), have been measured between two 3-mm-diameter copper pins, glued close to the notch edges by using Ag-filled epoxy. Accordingly, the technical fatigue crack initiation life can be defined as the number of loading cycles at which the normalized electrical potential $\Delta V/\Delta V_0$ shows a given increase, assumed here about equal to 1%.

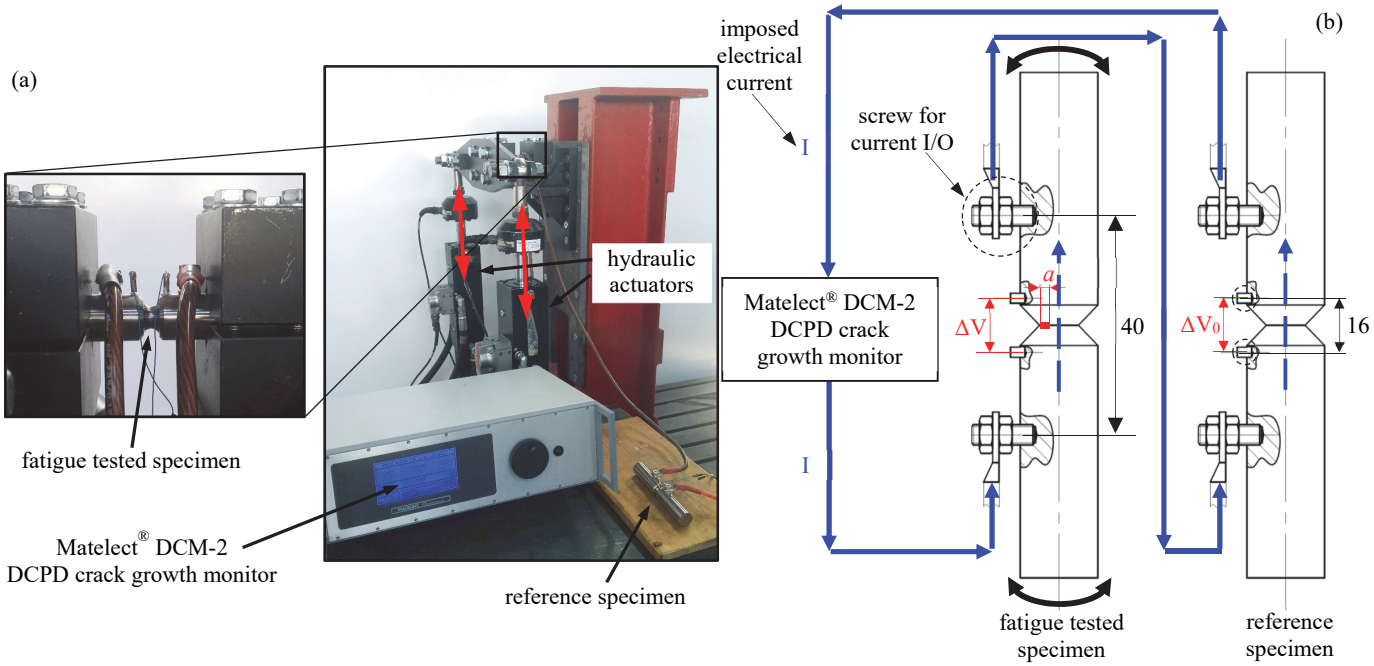

Figure 2: (a) Flexible test bench adopted for pure bending fatigue tests and (b) experimental setup of the adopted electrical potential drop measurement system.

CALIBRATION CURVES OF THE POTENTIAL DROP METHOD

According to the pioneering contributions by Ritchie and Bathe [17] and Aronson and Ritchie [18], the finite element method (FEM) is an accurate tool to derive the calibration curves of the electrical potential drop method, i.e. the potential drop as a function of the initiated crack depth in a specific specimen geometry, which is more simple and fast than experimental or theoretical calibrations.

The calibration curves relevant to Ti-6Al-4V notched specimens (reported in Fig. 1) have been derived by means of electrical FE analyses. The numerical analyses have been carried out using Ansys® code, by adopting a 3D, 10-node, tetrahedral, electric solid element (SOLID 232 of Ansys® element library). The boundary conditions have been applied to the FE model following the procedure extensively described in a previous contribution [19], which is not repeated here. However, in this case due to application of bending loadings in the fatigue tests, the fatigue crack has been assumed to initiate and subsequently to propagate with a semi-elliptical shape from the circumferential notch toward the center of the bar, and not concentrically as assumed in [19], in which axial and torsion loadings were considered.

The results obtained by employing a full 3D FE analysis relevant to Ti-6Al-4V notched specimens are reported in Figs. 3a in terms of ratio $\Delta V/\Delta V_0$ as a function of the normalized crack depth a/r_{net}, r_{net} being the radius of the net-section. A range of the ellipse semi-axes ratio c/a has been analysed, since it could be not the same in all specimens and it could also change during crack propagation as highlighted by Doremus et al. [20]. However, it is worth of mentioning that a saturation effect occurs on the calibration curves with increasing the c/a ratio, so that ratios higher than 4 have not been considered.

The calibration curves reported in Fig. 3a were used to define the crack initiation life in an operational manner, i.e. at a relative potential drop increase $\Delta V/\Delta V_0$ equal to 1.01. Such operational definition is consistent with that adopted by

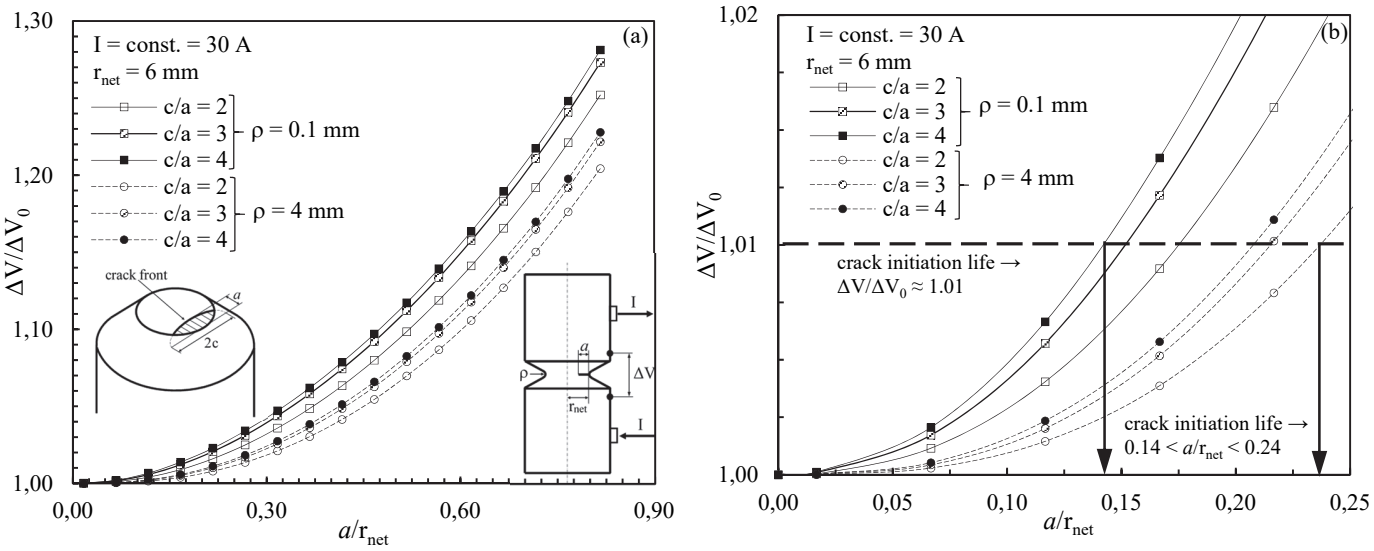

Figure 3: (a) Calibration curves $\Delta V/\Delta V_0$ obtained numerically as a function of the normalized crack depth a/r_{net}, for Ti-6Al-4V notched specimens. ΔV_0 represents the electrical potential of the reference un-cracked specimen (a = 0). (b) Definition of crack initiation life in terms of electrical potential drop.

Tanaka [6]. According to the zoom reported in Fig. 3b, it is seen that a ratio $\Delta V/\Delta V_0$ equal to 1.01 corresponds to a crack depth a in the range 0.8÷1.4 mm.

AVERAGED STRAIN ENERGY DENSITY APPROACH

The strain energy density (SED) averaged over a control volume, the radius of which is thought of as a material property according to Lazzarin and Zambardi [14], proved to efficiently account for notch effects both in static [14,21] and fatigue [14,22,23] structural strength problems. The idea is reminiscent of the stress averaging to perform along a material-dependent microstructural length, according to the approach proposed by Neuber.
Such a method was formalized and applied first to sharp, zero radius, V-notches [14] and later extended to blunt U and V-notches [15]. When dealing with sharp V-notches, see for example the case with ρ = 0.1 mm in Fig. 1, the control volume is a circular sector of radius R_0 centered at the notch tip [14] as shown in Fig. 4a. For a blunt V-notch, see for example the case with ρ = 4 mm in Fig. 1, the volume assumes the crescent shape shown in Fig. 4b [15], where R_0 is the depth measured along the notch bisector line. The outer radius of the crescent shape is equal to $R_0 + r_0$, where r_0 depends on the notch opening angle 2α and on the notch root radius ρ according to the following expression:

$$r_0 = \frac{q-1}{q}\rho \tag{1}$$

with q defined as:

$$q = \frac{2\pi - 2\alpha}{\pi} \tag{2}$$

The control radius R_0 for fatigue strength assessment of notched components made of titanium grade 5 alloy has been previously estimated by Berto et al. [24] by equating the averaged SED in two situations, i.e. the fatigue limit (or the high-cycle fatigue strength) of un-notched and notched specimens, respectively. Therefore, R_0 combines two material properties: the high-cycle fatigue strength of smooth specimens, referred to $N_A = 2 \cdot 10^6$ cycles, and the value of the Notch Stress Intensity Factor (NSIF) range for sharp V-notches with opening angle equal to 90 degrees, referred to the same number of cycles N_A, according to Eqs. (3) and (4) derived in [4,14]. Berto et al. obtained the following values for the

control radius R_0 of Ti-6Al-4V [24] dealing with tension (mode I) and torsion (mode III) loadings, respectively, with a load ratio R = -1:

$$R_{0,I} = \left(\sqrt{2e_1} \cdot \frac{\Delta K_{I,A}}{\Delta \sigma_A} \right)^{\frac{1}{1-\lambda_1}} = \left(\sqrt{2 \cdot 0.146} \cdot \frac{452\ \text{MPa} \cdot \text{mm}^{0.455}}{950\ \text{MPa}} \right)^{\frac{1}{1-0.545}} \rightarrow 0.051\text{mm} \quad (3)$$

$$R_{0,III} = \left(\sqrt{\frac{e_3}{1+\nu}} \cdot \frac{\Delta K_{III,A}}{\Delta \tau_A} \right)^{\frac{1}{1-\lambda_3}} = \left(\sqrt{\frac{0.310}{1+0.3}} \cdot \frac{1216\ \text{MPa} \cdot \text{mm}^{0.333}}{776\ \text{MPa}} \right)^{\frac{1}{1-0.666}} \rightarrow 0.449\text{mm} \quad (4)$$

It should be noted that the control radius R_0 for fatigue strength assessment of Ti-6Al-4V notched components assumes extremely different values under mode I and mode III, so that the energy contributions related to the two different loadings should be averaged in control volumes of different size [4]. The idea of a control volume size dependent on the loading mode has been proposed for the first time in [4] dealing with the multiaxial fatigue strength assessment of notched specimens made of 39NiCrMo3 steel, then it has been successfully applied also for the fatigue strength assessment of notched components made of AISI 416 [25] and cast iron EN-GJS400 [26] subjected to combined tension and torsional loading.

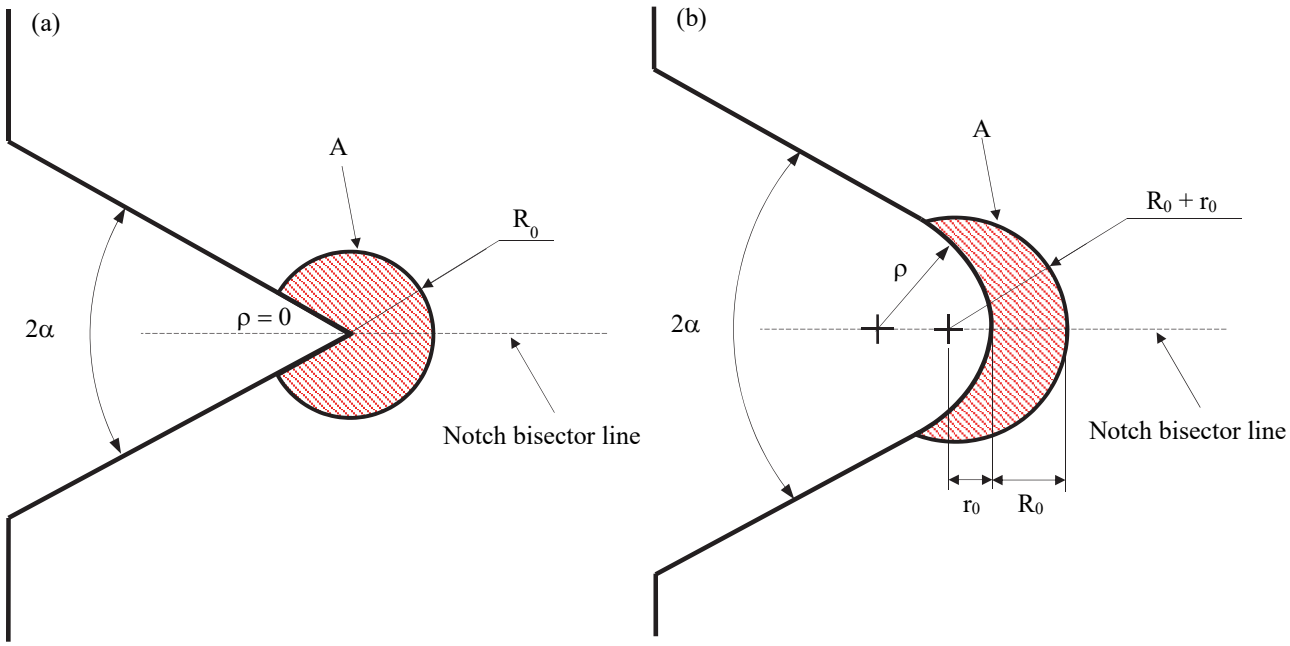

Figure 4: Control volume for specimens weakened by (a) sharp [14] and (b) blunt V-notches [15].

Once the size of the control volume is properly defined, the averaged SED can be evaluated directly from the FE results, $\Delta\overline{W}$, by summation of the strain-energies $W_{FEM,i}$ calculated for each i-th finite element belonging to the control volume V (or area A in two-dimensional problems, as shown in Fig. 4):

$$\Delta\overline{W} = c_W \frac{\sum_V W_{FEM,i}}{V} \quad (5)$$

where the coefficient c_w accounts for the effect of the nominal load ratio R [27], when the range value of the nominal stress is applied to the FE model. It is equal to 1 for R = 0 and to 0.5 for R = −1. Eq. (5) represents the so-called direct approach to calculate the averaged SED. According to a recent contribution of Lazzarin et al. [28], very coarse FE meshes can be adopted within the control volume (see Fig. 5).

SED-BASED REANALYSIS OF CRACK INITIATION AND TOTAL LIFE EXPERIMENTAL DATA

The local SED values, averaged over the control volume relevant to mode I loadings ($R_{0,I}$ = 0.051 mm), have been calculated using the direct approach, $\Delta\overline{W}$, according to Eq. (5) (with about 50 finite elements inside the control volume). Due to application of non axis-symmetric loadings, i.e. pure bending, 3D FE analyses of the cylindrical specimens were needed to evaluate the averaged SED. To obtain the 3D mesh, first, a 2D free mesh pattern of quadrilateral 8-node PLANE 183 elements has been generated; after that, the 2D FE mesh has been extruded about Y axis by using 3D 20-node brick elements (SOLID186 of the Ansys® element library) and by setting a proper extrusion step size in order to obtain a control volume V having both radius and depth equal to $R_{0,I}$, as suggested for 3D applications of the SED approach [21,23]. An example of the adopted FE mesh along with a detail of the structural volume for averaged SED calculation is reported in Fig. 5. It should be noted that only a quarter of each specimen has been modelled, taking advantage of the anti-symmetry on the YZ plane and of the symmetry on the XY plane (see Fig. 5). To properly simulate the loads and restraints applied by the adopted test bench (see Fig. 2a), the cylindrical surface highlighted in gray in Fig. 5a was fixed, while bending loading was applied by means of concentrated forces at the opposite end.

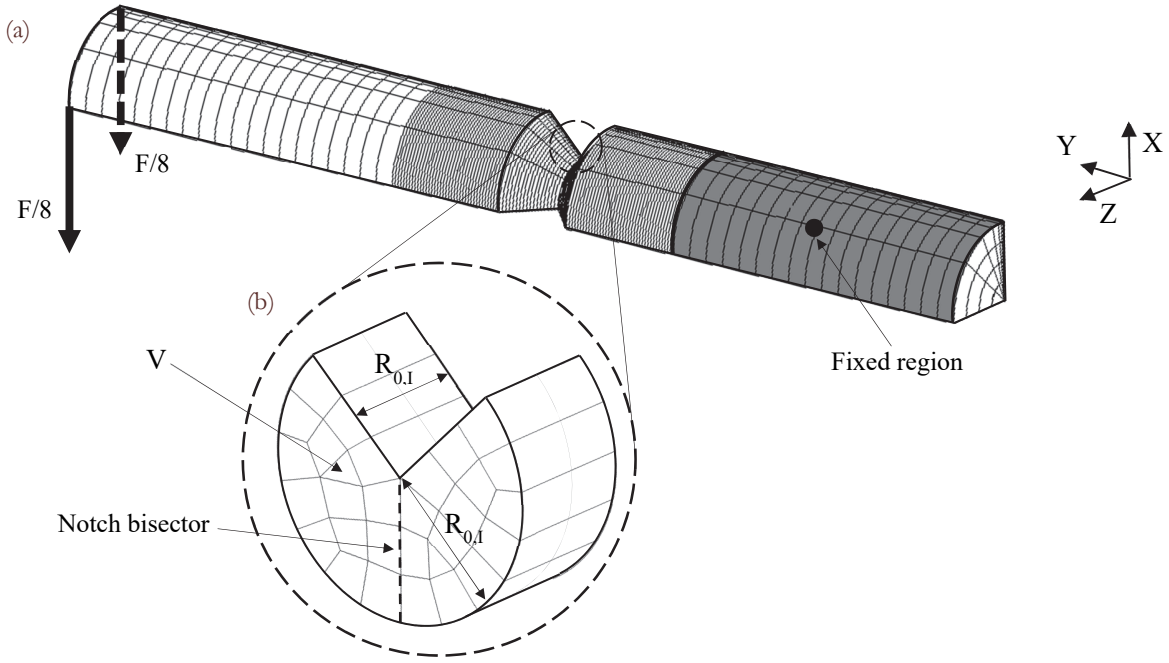

Figure 5: (a) Coarse FE mesh (about 50 FE inside the control volume) adopted in the 3D numerical analyses. The Y-axis coincides with the axis of the specimen. (b) Details of the FE mesh inside the control volume V. Considered case: sharp V-notched specimen (ρ = 0.1 mm) under pure bending loading, $R_{0,I}$ = 0.051 mm.

The preliminary experimental fatigue results presented in terms of local SED and relevant to pure bending fatigue loading are reported in Fig. 6a, where the operational definition of crack initiation life ($\Delta V/\Delta V_0$ = 1.01 according to Fig. 3b) has been applied. In a recent contribution of the present authors [16], it has been highlighted that a physical definition of the crack initiation life in relation to the SED-approach could be defined when the crack depth *a* equals the structural volume size R_0, that is the initiated crack depth leads to the structural volume failure. Dealing with the present results, it should be noted that: (i) given a crack depth *a*, the potential drop method is less sensitive to the initiation of an elliptical crack than to the initiation of a circumferential one (calibration curves of Fig. 3 should be compared with those reported in [19]); (ii) the control radius $R_{0,I}$ for fatigue strength assessment of Ti-6Al-4V notched components is equal to 0.051 mm. Therefore, the physical definition of the crack initiation life ($a = R_{0,I}$) corresponds to a relative potential drop increase $\Delta V/\Delta V_0$ lower than 1‰ (Fig. 3b): such a reduced $\Delta V/\Delta V_0$ value is not applicable to the present case due to the un-sufficiently high sensitivity of the adopted DCPD crack growth monitor device.

Leaving aside the physical definition of crack initiation, Fig. 6a shows that the ratio between crack initiation life according to the operational definition (open markers) and total life (filled markers) is equal to approximately 0.50÷0.60 for the sharp V-notch (ρ = 0.1 mm), while it is equal to about 0.90 for the blunt notch (ρ = 4 mm).
Fig. 6b shows a comparison between the averaged SED-based scatter-band calibrated previously by Berto el al. [24] on about 160 uniaxial and multiaxial experimental data obtained from sharp V-notched Ti-6Al-4V specimens and the new fatigue results relevant to pure bending loading, obtained in the present contribution and expressed in terms of total fatigue life. It can be observed from Fig. 6b that all new data fall within the SED-based scatter band showing a good agreement between theoretical estimations and experimental results. However, it should be noted that the averaged SED-based scatter-band reported in Fig. 6b is characterized by a rather wide scatter (T_W = 2.50, i.e. an equivalent stress-based scatter index $T_\sigma = \sqrt{T_W}$ = 1.58), being calibrated on experimental data expressed in terms of total fatigue life. It is worth noting that Fig. 6a suggests that the scatter index could be reduced if the averaged SED-based scatter-band was calibrated on crack initiation data rather than total fatigue life data.

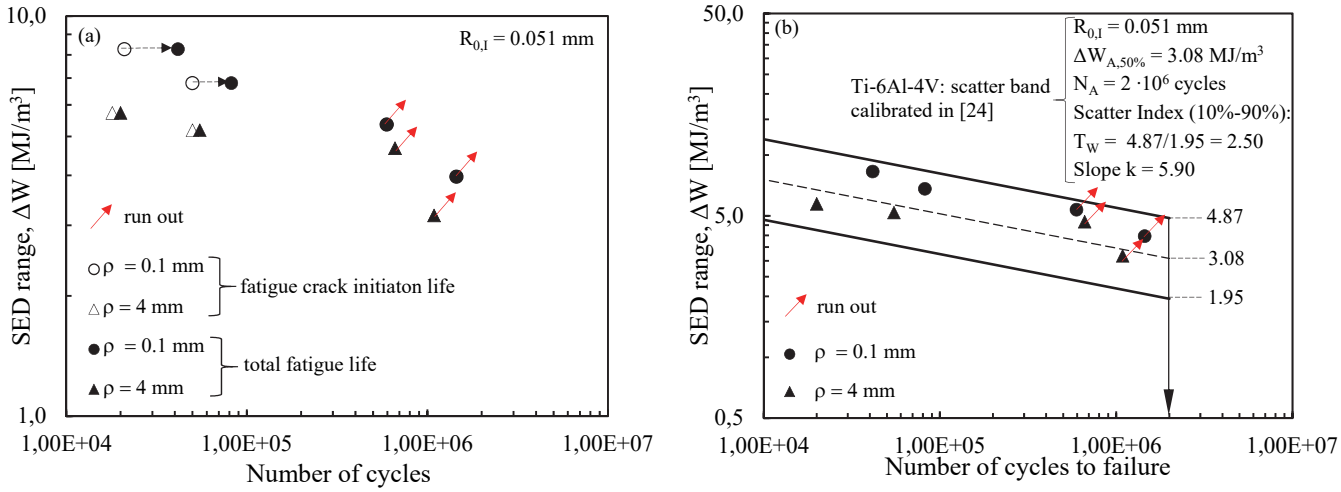

Figure 6: (a) Crack initiation (open markers) and fatigue life to failure (filled markers) of Ti-6Al-4V notched specimens expressed in terms of averaged SED. (b) Comparison of new fatigue data in terms of total fatigue life with the averaged SED-based scatter-band calibrated previously [24] on about 160 uniaxial and multiaxial experimental fatigue results obtained from sharp V-notched specimens.

Conclusions

In the present contribution, some preliminary experimental fatigue results, obtained from circumferentially notched specimens made of titanium alloy, Ti-6Al-4V, with different notch root radii and subjected to pure bending fatigue loadings, have been reanalysed by means of the averaged strain energy density (SED) approach. Agreement has been found between new fatigue data and a SED-based scatter band previously calibrated on uniaxial and multiaxial fatigue results in terms of total fatigue life. However, if the crack initiation life had been considered, even though defined in an operational manner, reduction of scattering in the SED-based synthesis of notches of different severity is likely to be obtained and it will be the subject of future investigations.

References

[1] Tanaka, K., Hashimoto, A., Narita, J., Egami, N., Fatigue life of circumferentially notched bars of austenitic stainless steel under cyclic torsion with and without static tension, J. Soc. Mater. Sci. Jpn., 58 (2009) 1044–1050.
[2] Tanaka, K., Small fatigue crack propagation in notched components under combined torsional and axial loading, Procedia Eng., 2 (2010) 27–46. DOI: 10.1016/j.proeng.2010.03.004.
[3] Ohkawa, C., Ohkawa, I., Notch effect on torsional fatigue of austenitic stainless steel: Comparison with low carbon steel, Eng. Fract. Mech., 78 (2011) 1577–1589. DOI:10.1016/j.engfracmech.2011.01.015.
[4] Berto, F., Lazzarin, P., Yates, J.R., Multiaxial fatigue of V-notched steel specimens: A non-conventional application of the local energy method, Fatigue Fract. Eng. Mater. Struct., 34 (2011) 921–943.

[5] Okano, T., Hisamatsu, N., Effect of notch of torsional fatigue property of pure titanium, Proc. 31 Symp. Fatigue, Soc. Mater. Sci. Japan, 31 (2012) 129–133.
[6] Tanaka, K., Crack initiation and propagation in torsional fatigue of circumferentially notched steel bars, Int. J. Fatigue, 58 (2014) 114–125. DOI: 10.1016/j.ijfatigue.2013.01.002.
[7] Atzori, B., Berto, F., Lazzarin, P., Quaresimin, M., Multi-axial fatigue behaviour of a severely notched carbon steel, Int. J. Fatigue, 28 (2006) 485–493. DOI: 10.1016/j.ijfatigue.2005.05.010.
[8] Tanaka, K., Ishikawa, T., Narita, J., Egami, N., Fatigue life of circumferentially notched bars of carbon steel under cyclic torsion with and without static tension, J. Soc. Mater. Sci. Jpn, 60 (2011).
[9] Ritchie, R.O., McClintock, F.A., Nayeb-Hashemi, H., Ritter, M.A., Mode III fatigue crack propagation in low alloy steel, Metall. Trans. A, 13 (1982) 101–110. DOI: 10.1007/BF02642420.
[10] Tschegg, E.K., A contribution to mode III fatigue crack propagation, Mater. Sci. Eng., 54 (1982) 127–136. DOI: 10.1016/0025-5416(82)90037-4.
[11] Tschegg, E.K., The influence of the static I load mode and R ratio on mode III fatigue crack growth behaviour in mild steel, Mater. Sci. Eng. 59 (1983) 127–137. DOI:10.1016/0025-5416(83)90094-0.
[12] Tanaka, K., Akiniwa, Y., Nakamura, H., J-integral approach to mode III fatigue crack propagation in steel under torsional loading, Fatigue Fract. Eng. Mater. Struct., 19 (1996) 571–579. DOI: 10.1111/j.1460-2695.1996.tb00993.x.
[13] Yu, H., Tanaka, K., Akiniwa, Y., Estimation of torsional fatigue strength of medium carbon steel bars with a circumferential crack by the cyclic resistance-curve method, Fatigue Fract. Eng. Mater. Struct., 21 (1998) 1067–1076, DOI: 10.1046/j.1460-2695.1998.00105.x.
[14] Lazzarin, P., Zambardi, R., A finite-volume-energy based approach to predict the static and fatigue behavior of components with sharp V-shaped notches, Int. J. Fract., 112 (2001) 275–298. DOI:10.1023/A:1013595930617.
[15] Lazzarin, P., Berto, F., Some expressions for the strain energy in a finite volume surrounding the root of blunt V-notches, Int. J. Fract., 135 (2005) 161–185. DOI: 10.1007/s10704-005-3943-6.
[16] Campagnolo, A., Meneghetti, G., Berto, F., Tanaka, K., Crack initiation life in notched steel bars under torsional fatigue: Synthesis based on the averaged strain energy density approach, Int. J. Fatigue, 100 (2017) 563-574. DOI: 10.1016/j.ijfatigue.2016.12.022.
[17] Ritchie, R.O., Bathe, K.J., On the calibration of the electrical potential technique for monitoring crack growth using finite element methods, Int. J. Fract., 15 (1979) 47–55, DOI: 10.1007/BF00115908.
[18] Aronson, G., Ritchie, R., Optimization of the Electrical Potential Technique for Crack Growth Monitoring in Compact Test Pieces Using Finite Element Analysis, J. Test. Eval., 7 (1979) 208. DOI: 10.1520/JTE11382J.
[19] Campagnolo, A., Meneghetti, G., Berto, F., Tanaka, K., Averaged strain energy density-based synthesis of crack initiation life of notched titanium and steel bars under uniaxial and multiaxial fatigue, Fatigue 2017, Cambridge, UK: (2017).
[20] Doremus, L., Nadot, Y., Henaff, G., Mary, C., Pierret, S., Calibration of the potential drop method for monitoring small crack growth from surface anomalies – Crack front marking technique and finite element simulations, Int. J. Fatigue, 70 (2015) 178–185. DOI: 10.1016/j.ijfatigue.2014.09.003.
[21] Berto, F., Lazzarin, P., Recent developments in brittle and quasi-brittle failure assessment of engineering materials by means of local approaches, Mater. Sci. Eng. R Reports, 75 (2014) 1–48. DOI: 10.1016/j.mser.2013.11.001.
[22] Livieri, P., Lazzarin, P., Fatigue strength of steel and aluminium welded joints based on generalised stress intensity factors and local strain energy values, Int. J. Fract., 133 (2005) 247–276. DOI: 10.1007/s10704-005-4043-3.
[23] Berto, F., Campagnolo, A., Chebat, F., Cincera, M., Santini, M., Fatigue strength of steel rollers with failure occurring at the weld root based on the local strain energy values: modelling and fatigue assessment, Int. J. Fatigue, 82 (2016) 643–657. DOI: 10.1016/j.ijfatigue.2015.09.023.
[24] Berto, F., Campagnolo, A., Lazzarin, P., Fatigue strength of severely notched specimens made of Ti-6Al-4V under multiaxial loading, Fatigue Fract. Eng. Mater. Struct., 38 (2015) 503–517.
[25] Berto, F., Lazzarin, P., Fatigue strength of structural components under multi-axial loading in terms of local energy density averaged on a control volume, Int. J. Fatigue, 33 (2011) 1055–1065. DOI: 10.1016/j.ijfatigue.2010.11.019.
[26] Berto, F., Lazzarin, P., Tovo, R., Multiaxial fatigue strength of severely notched cast iron specimens, Int. J. Fatigue, 67 (2014) 15–27. DOI: 10.1016/j.ijfatigue.2014.01.013.
[27] Lazzarin, P., Sonsino, C.M., Zambardi, R., A notch stress intensity approach to assess the multiaxial fatigue strength of welded tube-to-flange joints subjected to combined loadings, Fatigue Fract. Eng. Mater. Struct., 27 (2004) 127–140.
[28] Lazzarin, P., Berto, F., Zappalorto, M., Rapid calculations of notch stress intensity factors based on averaged strain energy density from coarse meshes: Theoretical bases and applications, Int. J. Fatigue, 32 (2010) 1559–1567. DOI: 10.1016/j.ijfatigue.2010.02.017.